Autophagy-related protein Vps34 controls the homeostasis and function of antigen cross-presenting CD8α$^+$ dendritic cells

Vrajesh V. Parekh[a,1], Sudheer K. Pabbisetty[a], Lan Wu[a], Eric Sebzda[a], Jennifer Martinez[b], Jianhua Zhang[c,d], and Luc Van Kaer[a,2]

[a]Department of Pathology, Microbiology and Immunology, Vanderbilt University School of Medicine, Nashville, TN 37232; [b]Immunity, Inflammation, and Disease Laboratory, National Institute of Environmental Health Sciences, Research Triangle Park, NC 27709; [c]Department of Pathology, University of Alabama at Birmingham, Birmingham, AL 35294; and [d]Birmingham Veterans Affairs Medical Center, Birmingham, AL 35233

Edited by Kenneth M. Murphy, Washington University, St. Louis, MO, and approved June 23, 2017 (received for review April 20, 2017)

The class III PI3K Vacuolar protein sorting 34 (Vps34) plays a role in both canonical and noncanonical autophagy, key processes that control the presentation of antigens by dendritic cells (DCs) to naive T lymphocytes. We generated DC-specific *Vps34*-deficient mice to assess the contribution of Vps34 to DC functions. We found that DCs from these animals have a partially activated phenotype, spontaneously produce cytokines, and exhibit enhanced activity of the classic MHC class I and class II antigen-presentation pathways. Surprisingly, these animals displayed a defect in the homeostatic maintenance of splenic CD8α$^+$ DCs and in the capacity of these cells to cross-present cell corpse-associated antigens to MHC class I-restricted T cells, a property that was associated with defective expression of the T-cell Ig mucin (TIM)-4 receptor. Importantly, mice deficient in the Vps34-associated protein Rubicon, which is critical for a noncanonical form of autophagy called "Light-chain 3 (LC3)-associated phagocytosis" (LAP), lacked such defects. Finally, consistent with their defect in the cross-presentation of apoptotic cells, DC-specific *Vps34*-deficient animals developed increased metastases in response to challenge with B16 melanoma cells. Collectively, our studies have revealed a critical role of Vps34 in the regulation of CD8α$^+$ DC homeostasis and in the capacity of these cells to process and present antigens associated with apoptotic cells to MHC class I-restricted T cells. Our findings also have important implications for the development of small-molecule inhibitors of Vps34 for therapeutic purposes.

antigen presentation | dendritic cells | Vps34 | MHC class I | cross-presentation

Dendritic cells (DCs) play a central role in the activation of naive T cells and direct the induction of adaptive immune responses against invading microorganisms. These cells capture foreign and self antigens and present them to MHC class I- and class II-restricted CD8$^+$ and CD4$^+$ T cells, respectively. MHC class II-associated peptides are typically generated by proteolysis of endocytosed proteins (1), whereas MHC class I-associated peptides are predominantly generated by proteolysis of cytosolic proteins (2). However, in specialized antigen-presenting cells (APCs) such as a DC subset expressing CD8α and CD103, extracellular antigens can be presented in the context of MHC class I molecules via a cross-presentation pathway whose mechanism is incompletely understood (3).

In recent years, the process of autophagy has been implicated in controlling antigen processing (4). Autophagy is a conserved catabolic process that maintains cellular energy homeostasis in response to a wide spectrum of cellular stresses (5, 6). Autophagy ensures continuous degradation of long-lived proteins, damaged cellular organelles, and protein aggregates to facilitate recycling of nutrients and hence promote cellular metabolism. The formation of autophagosomes requires an interplay between autophagy-related (Atg) gene products, which have been well characterized in yeast and are conserved in mammals (7). Defective autophagy in mammalian cells results in the accumulation of damaged cellular organelles and protein aggregates, leading to stress with pathological consequences (8). Autophagy has common features with endocytosis, with which it shares effector molecules (9). However, how these processes and their shared machinery regulate antigen presentation remains incompletely understood.

Vacuolar protein sorting 34 (Vps34) is a class III PI3K that plays a role in endocytosis, intracellular vesicular trafficking, and autophagosome formation during autophagy (10). *Vps34*-deficient cells display defective autophagic flux leading to the accumulation of aggregated cellular proteins and organelles, and *Vps34* ablation in mice causes significant pathology (11–14). Although Vps34 forms multiple protein complexes that mediate its diverse cellular functions in canonical autophagy, noncanonical autophagy, and endocytosis (15), it is unclear which of these processes is responsible for the phenotypes observed in *Vps34*-deficient cells and mice.

In the present study, we generated mice with a DC-specific deletion of *Vps34* to determine its effects on DC functions such as antigen presentation and priming of adaptive immune responses. Our findings revealed a critical role for Vps34 in the homeostasis and function of DCs that is dependent on the canonical autophagy pathway.

Results

DC-Specific *Vps34*-Deficient Mice Exhibit a Selective Reduction in CD8α$^+$ DCs. We generated *Vps34*$^{f/f}$;*CD11c-Cre* mice, which exhibited selective *Vps34* ablation in DCs (Fig. S1). Although these mice displayed no signs of disease and were grossly indistinguishable

Significance

Dendritic cells (DCs) of the immune system are critical for displaying foreign antigens to T lymphocytes, a process called "antigen presentation." This process may involve Vacuolar protein sorting 34 (Vps34), a protein implicated in diverse cellular processes, including endocytosis, an extracellular product uptake system, and autophagy, an intracellular degradation system. Here we have generated and analyzed mice in which the *Vps34* gene is specifically knocked out in DCs. These animals displayed defects in the survival and function of a subset of DCs specialized in presenting antigens from dead cells to T cells. Thus our findings have revealed a critical contribution of Vps34 in DC functions that may have important implications for targeting this pathway for therapeutic purposes.

Author contributions: V.V.P., S.K.P., E.S., and L.V.K. designed research; V.V.P., S.K.P., and L.W. performed research; J.M. and J.Z. contributed new reagents/analytic tools; V.V.P., S.K.P., E.S., J.M., J.Z., and L.V.K. analyzed data; and V.V.P. and L.V.K. wrote the paper.

The authors declare no conflict of interest.

This article is a PNAS Direct Submission.

[1]Present address: Pfizer Inc., San Diego, CA 92121.

[2]To whom correspondence should be addressed. Email: luc.van.kaer@vanderbilt.edu.

This article contains supporting information online at www.pnas.org/lookup/suppl/doi:10.1073/pnas.1706504114/-/DCSupplemental.

from control littermates, their lymphoid organs were visibly enlarged compared with control animals (Fig. 1*A*), and lymphoid cellularity was increased (Fig. 1*B*).

Conventional DCs in lymphoid organs are a heterogeneous population of CD11b^{int}CD11c^{hi} cells that can be further subdivided into populations expressing CD8α and CD103 (16). Although we found no differences in the frequency of total DCs (Fig. 1*C*), the absolute numbers of DCs were significantly increased in the lymphoid organs of *Vps34*$^{f/f}$;*CD11c-Cre* mice (Fig. 1*C*). The prevalence of the DC population expressing CD103 and CD8α in *Vps34*$^{f/f}$;*CD11c-Cre* mice was sharply reduced (Fig. 1 *D* and *E*), although absolute numbers were comparable in both groups of mice (Fig. 1*E*). CD11b^{-}CD103^{+} cells are a major population of DCs in the lungs (17) that are developmentally related to conventional CD8α^{+} DCs in the spleen (16). We observed a trend for reduced frequency of such DCs in the lungs of *Vps34*$^{f/f}$;*CD11c-Cre* mice (Fig. 1 *F* and *G*). The frequency of other populations of myeloid cells, including CD11b^{hi}CD11c^{-} and CD11b^{int}CD11c^{int} cells, was similar in the two groups of mice (Fig. S2). Immunophenotyping of lymphocytes revealed that the frequencies of CD4^{+} and CD8^{+} T cells, B cells, and natural killer (NK) cells were similar in the two groups of mice, but absolute numbers of these cells were profoundly increased in *Vps34*$^{f/f}$;*CD11c-Cre* mice (Fig. S3). Thus, these data suggest that the increased numbers of DCs in the lymphoid organs of *Vps34*$^{f/f}$;*CD11c-Cre* mice are associated with concomitant increases in T, B, and NK cells, thereby increasing the overall cellularity and size of the lymphoid organs.

To determine if the selective reduction of CD8α^{+} DCs in the spleen is related to defects in their development or homeostasis, we analyzed young mice that contained comparable numbers of cells, suggesting normal DC development (Fig. 1*H*). To determine if the loss of CD8α^{+} DCs in older mice was cell intrinsic,

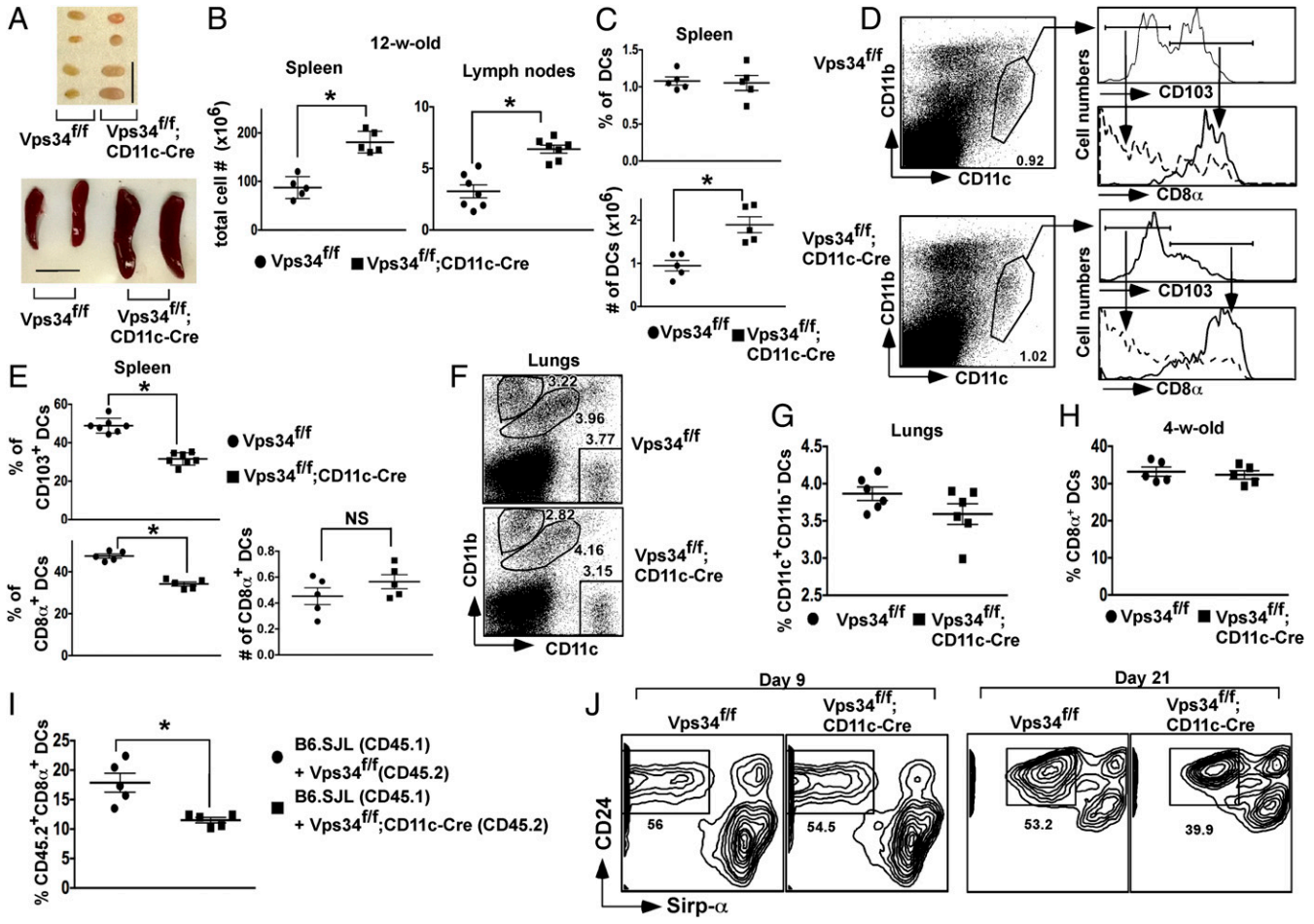

Fig. 1. DC subpopulations in *Vps34*$^{f/f}$;*CD11c-Cre* mice. (*A*) Spleens and a pair of inguinal lymph nodes from representative 12-wk-old *Vps34*$^{f/f}$ and *Vps34*$^{f/f}$;*CD11c-Cre* mice are shown. (Scale bar, 1 cm.) (*B*) Single-cell suspensions of spleens and a pair of inguinal lymph nodes were prepared and counted. Results from three independent experiments (five to seven animals per group) are shown. *$P < 0.001$. (*C*) Percent and absolute numbers of DCs in the spleen and lymph nodes of *Vps34*$^{f/f}$ or *Vps34*$^{f/f}$;*CD11c-Cre* mice. Results from three independent experiments (five to seven animals per group) are shown. *$P < 0.01$. (*D*) Splenocytes from 12-wk-old *Vps34*$^{f/f}$ or *Vps34*$^{f/f}$;*CD11c-Cre* mice were stained with anti-CD11c, -CD103, -CD8α, and -CD11b antibodies. The CD11c^{hi}CD11b^{lo} cells were evaluated for CD103 expression, and levels of CD8α on CD103^{-} and CD103^{+} cells were measured. (*E*) Summary of the percentage and absolute numbers of CD103- or CD8α-expressing DCs in the spleen. Pooled results from two independent experiments (five to seven mice in each group) are shown. *$P < 0.01$. (*F* and *G*) Single-cell suspensions of lungs from the indicated mice were stained with anti-CD11c, -CD103, -CD8α, and -CD11b antibodies. A representative experiment (*F*) and a summary of the data pooled from two independent experiments (six mice in each group) (*G*) are shown. (*H*) Frequency of CD8α^{+} DCs in 4-wk-old mice. (*I*) Bone marrow chimeras were generated in lethally irradiated B6 mice (CD45.2) by transfer of 10^7 cells bone marrow cells from wild-type B6.SJL mice (CD45.1) and *Vps34*$^{f/f}$;*CD11c-Cre* (CD45.2) or *Vps34*$^{f/f}$ (CD45.2) mice mixed at a 1:1 ratio. At the end of 12 wk spleen cells from the chimeric mice were tested for the frequency of CD8α^{+} cells among CD45.2^{+} DCs. A summary of two independent experiments (five mice per group) is shown. *$P < 0.05$. (*J*) Bone marrow-derived Flt3L-driven DCs were generated in the presence of 150 ng/mL of rFlt3L for 9–21 d of in vitro culture. Cells analogous to splenic CD8α^{+} DCs were identified as CD45RA^{-}CD24^{+}Sirp-α^{-} cells. Representative plots from three individual experiments with two mice per group are shown.

we generated mixed bone marrow chimeras using wild-type and *Vps34*$^{f/f}$;*CD11c-Cre* or *Vps34*$^{f/f}$ bone marrow cells. We found a selective reduction in *Vps34*-deficient CD8α$^+$ DCs (Fig. 1*I*), indicating that Vps34 is required for the normal homeostatic maintenance of CD8α$^+$ DCs. To validate these results further, we differentiated Flt3L-driven bone marrow-derived DCs (BMDCs) in vitro and analyzed CD45RA$^-$CD24$^+$Sirp-α$^-$ DCs, which are considered analogous to CD8α$^+$ DCs in the spleen (18). We found that this population of DCs from *Vps34*$^{f/f}$;*CD11c-Cre* mice was present at normal levels early (day 9) after culture but was reduced at a later time point (day 21) compared with the control cultures (Fig. 1*J*). Despite differences in the timing of DC development in vitro vs. in vivo, these findings are consistent with defects in DC homeostasis rather than development.

Spontaneous DC Activation in *Vps34*$^{f/f}$;*CD11c-Cre* Mice. We next assessed the DC activation status during steady-state conditions and found that *Vps34*-deficient DCs expressed modestly increased levels of CD40 and MHC class I and class II molecules but not CD80 or CD86, suggesting a partially activated state (Fig. 2*A*). Additionally, we found that *Vps34*-deficient DCs spontaneously secrete copious amounts of both pro- and anti-inflammatory cytokines such as TNFα, IL-6, and IL-10 (Fig. 2*B*), as is consistent with a prior study performed in vitro with a small-molecule inhibitor of Vps34, SAR405 (19). Upon activation with Toll-like receptor (TLR) ligands, no substantial enhancement of cytokine secretion by *Vps34*-deficient DCs was observed compared with control DCs. We obtained similar results for activated BMDCs, but these cells did not spontaneously produce cytokines (Fig. 2 *C* and *D*), perhaps because of the lack of continuous exposure to TLR ligands, as may be the case for splenic DCs in vivo. Collectively, these results indicate that DCs from *Vps34*$^{f/f}$;*CD11c-Cre* mice exhibit a partially activated phenotype with spontaneous production of both pro- and anti-inflammatory cytokines.

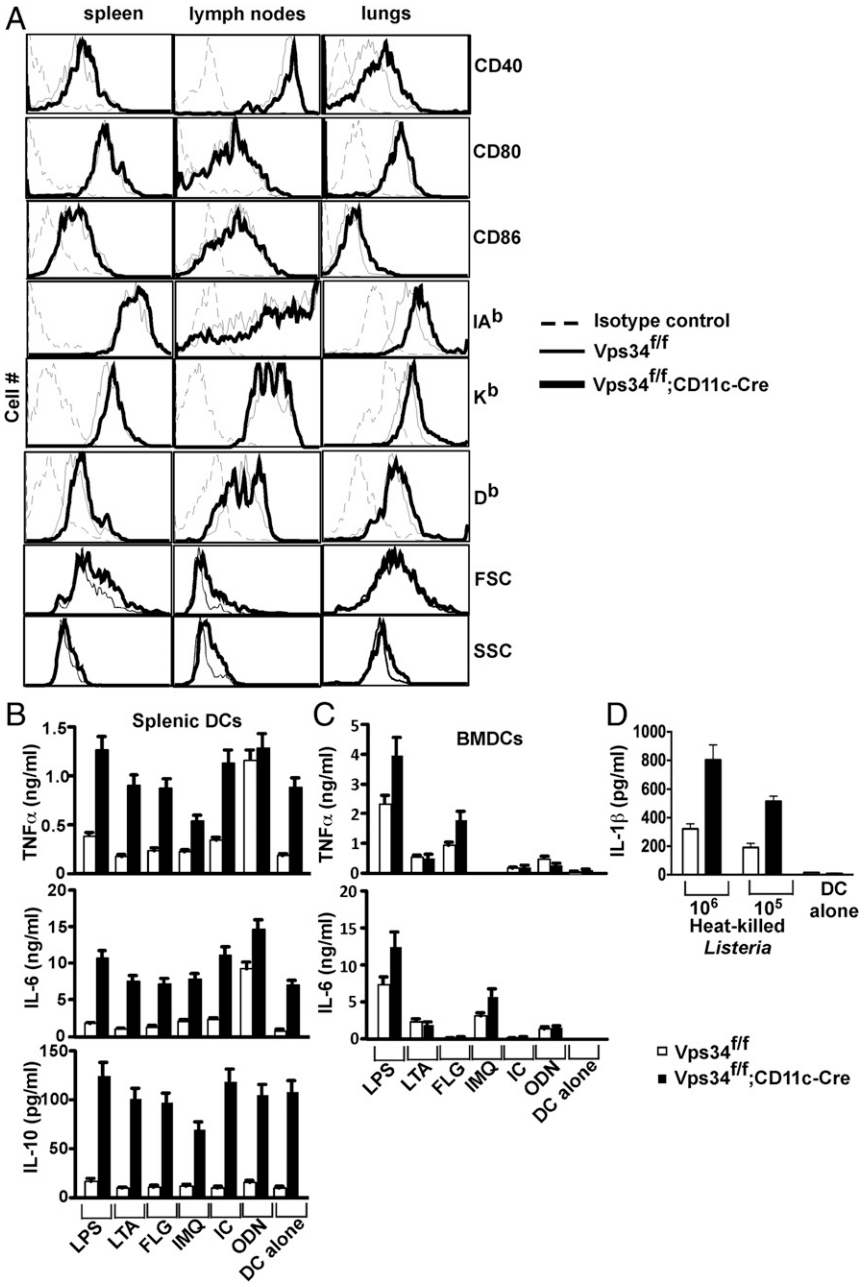

Fig. 2. Spontaneous DC activation in *Vps34*$^{f/f}$;*CD11c-Cre* mice. (*A*) Splenocytes, lymph node, and lung cells were prepared from mice, stained with anti-CD11c and -CD11b antibodies and with anti-CD40, -CD80, -CD86, -K^b, -D^b, or isotype control antibodies, and were analyzed by flow cytometry. Representative plots from at least two experiments with six mice per group are shown. (*B*) Splenic DCs were purified by FACS and cultured in complete medium either alone or in the presence of the indicated stimuli for 24 h. Culture supernatants were collected to measure IL-6, TNFα, and IL-10 by cytometric bead array (CBA). A representative of three experiments is shown. The error bars indicate the mean ± SD of triplicate wells. (*C*) BMDCs were activated as in *B*, and culture supernatants were collected at 48 h for measurement of IL-6 and TNFα by CBA. A representative of three experiments is shown. The error bars indicate the mean ± SD of triplicate wells. (*D*) BMDCs (10^4 cells) were activated with the indicated numbers of heat-killed *L. monocytogenes* in a 24-well plate, and 48 h later culture supernatants were tested for IL-1β secretion by DCs. A representative of three experiments is shown. The error bars indicate the mean ± SD of triplicate wells.

Enhancement of the Classic MHC Class I and Class II Antigen-Presentation Pathways. Because autophagy has been implicated in antigen presentation (4), we analyzed this function of *Vps34*-deficient DCs. These cells were as effective as wild-type DCs in presenting an ovalbumin (OVA)-derived peptide to H-2K^b–restricted OT-I T cells (Fig. 3 *A* and *B*). However, *Vps34*-deficient DCs exhibited enhanced capacity to present cytoplasmic OVA antigens to OT-I cells (Fig. 3*B*). We repeated this experiment with sorted CD8α$^+$ and CD8α$^-$ DC populations and found that both subsets of *Vps34*-deficient DCs exhibited enhanced antigen presentation (Fig. 3 *C* and *D*). We obtained comparable results with BMDCs (Fig. 3*E*). Similarly, *Vps34*-deficient DCs showed enhanced capacity to present immunodominant lymphocytic choriomeningitis virus (LCMV) epitopes to cytotoxic T lymphocyte (CTL) lines (Fig. 3*F*). To test whether the partially activated phenotype of *Vps34*-deficient DCs plays a role, we activated purified splenic DCs with reagents that up-regulate MHC class I expression. We found that IFN-γ enhanced up-regulation of MHC class I (but not MHC class II) expression (Fig. S4) on *Vps34*-deficient DCs compared with control cells (Fig. 3 *G* and *H*), suggesting that the partially activated phenotype of *Vps34*-deficient DCs renders them even more sensitive to IFN-γ–mediated up-regulation of MHC class I and its associated antigen-processing machinery.

Next, we evaluated the MHC class II antigen-processing pathway. We found that *Vps34*-deficient and wild-type DCs had similar capacity to present an OVA-derived peptide to OT-II

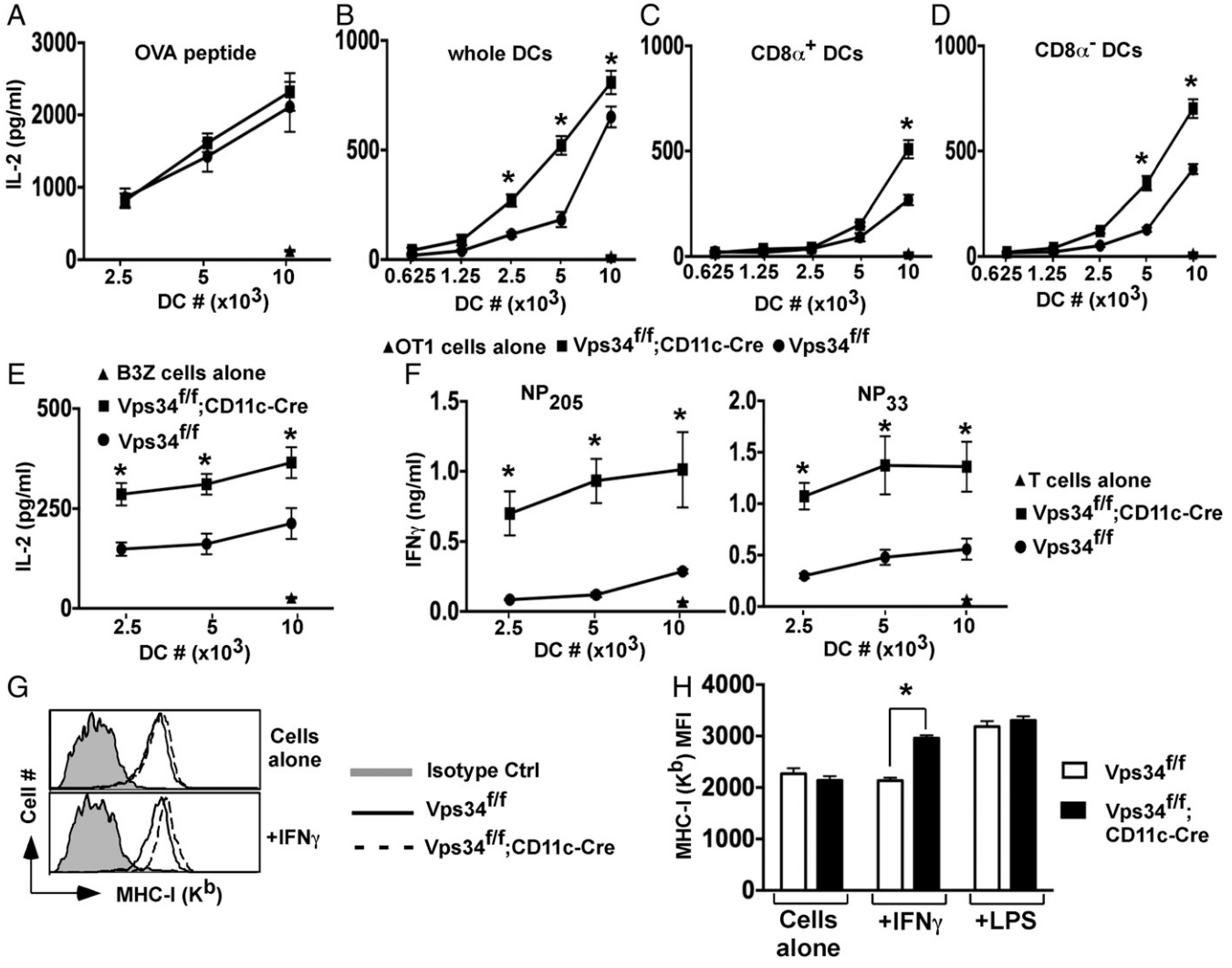

Fig. 3. Effects of *Vps34* deficiency on the classic MHC class I antigen-presentation pathway in DCs. (*A*) Splenic DCs were pulsed with MHC class I-restricted OVA peptides for 1 h in complete medium and were washed, OT-I T cells were added, and culture supernatants were collected after 24 h to measure IL-2 by CBA. Representative plots from two experiments with four mice per group are shown. (*B*) Total splenic DCs were loaded intracellularly with OVA protein by osmotic shock, washed, and cultured with 2×10^5 OT-I T cells, and culture supernatants were collected at 24 h for measurement of IL-2. (*C* and *D*) Splenic CD8α$^+$ (*C*) and CD8α$^-$ (*D*) DCs were sorted from the indicated mice, intracellularly loaded with OVA, and cultured with OT-I T cells for 24 h. IL-2 was measured in the culture supernatant. A representative of three experiments is shown. The error bars indicate the means ± SD of triplicate wells. *$P < 0.05$. (*E*) BMDCs were loaded with OVA by osmotic shock and cocultured with 2×10^4 B3Z hybridoma cells overnight, and then IL-2 in the supernatant was measured. Representative graphs from two experiments with four mice per group are shown. The error bars indicate the means ± SD of triplicate wells. *$P < 0.05$. (*F*) Splenic DCs (2×10^4) were infected with LCMV for 3 h, washed, and cultured with 2×10^5 cells of short-term CD8$^+$ T-cell lines specific for the LCMV-derived nucleoprotein peptides NP$_{205}$ or NP$_{33}$ for 36 h. The culture supernatants were collected, and IFN-γ was measured by ELISA. Representative graphs from three experiments with five mice per group are shown. Error bars indicate the means ± SD of triplicate wells. *$P < 0.05$. (*G* and *H*) Total splenic DCs were purified and stimulated with or without 15 ng/mL of IFN-γ or 1 μg/mL of LPS for 16 h. MHC class I (K^b) was measured by flow cytometry. A representative plot (*G*) and a summary of results pooled from three separate experiments (*H*) are shown. *$P < 0.01$.

T cells (Fig. 4*A*), but *Vps34*-deficient DCs showed an enhanced capacity to present soluble OVA protein (Fig. 4*B*). This finding was true for both the CD8α$^+$ and CD8α$^-$ DC subsets (Fig. 4 *C* and *D*). Similar results were obtained for BMDCs (Fig. 4 *E* and *F*). To determine whether the observed differences in MHC class II-restricted antigen presentation were to the result of the role of Vps34 in endocytosis, we tested the capacity of *Vps34*-deficient and wild-type BMDCs to endocytose particulate matter (fluorescent microbeads), soluble proteins (chimeric Eα-GFP protein), and bacteria (*Citrobacter rodentium*) in the presence or absence of the phagocytosis inhibitor cytochalasin D. We found that *Vps34*-deficient DCs exhibited modestly reduced uptake (Fig. S5), suggesting that these cells do not possess a major inherent defect in endocytosis or phagocytosis.

Defective Cell Corpse-Associated Antigen Cross-Presentation. In addition to presenting endogenous antigens on MHC class I molecules, CD8α$^+$ DCs can present exogenous antigens to MHC class I-restricted T cells in a process called "cross-presentation" (20). We sorted CD8α$^+$ and CD8α$^-$ DCs to measure their capacity to cross-present the model antigen OVA delivered in four different forms: soluble, targeted to DCs with anti-DEC205 antibodies, expressed by *Listeria monocytogenes* bacteria, and contained by apoptotic cells. We found that *Vps34*-deficient CD8α$^+$ DCs were equally as efficient as wild-type DCs in cross-presenting free OVA (Fig. 5*A*), OVA delivered to DCs via DEC205 (Fig. 5*B*), and OVA produced by *L. monocytogenes* (Fig. 5*C*). In sharp contrast, *Vps34*-deficient DCs displayed a marked defect in cross-presenting OVA antigens associated with apoptotic cells (Fig. 5*D*). Next, we measured cross-presentation of OVA-associated cell corpses in vivo after mice were injected with OVA-loaded, sublethally irradiated *TAP*$^{-/-}$ splenocytes and demonstrated a profound defect in *Vps34*$^{f/f}$;*CD11c-Cre* mice (Fig. 5*E*). Collectively, these results showed that *Vps34*-deficient DCs possess a competent cross-presentation pathway, but their capacity to cross-present cell corpse-associated antigens is impaired.

Defective Uptake of Cell Corpses Correlates with Reduced T-Cell Ig Mucin-4 Expression. We next explored the mechanism of defective cross-presentation of apoptotic cells by *Vps34*-deficient DCs. First, we determined the capacity of DCs to take up apoptotic cells in vivo and in vitro. For in vivo experiments, we injected sublethally irradiated splenocytes into groups of *Vps34*$^{f/f}$;*CD11c-Cre* and *Vps34*$^{f/f}$ mice and found that *Vps34*-deficient CD8α$^+$ DCs were defective in taking up apoptotic cells (Fig. 6 *A* and *B*). A similar apoptotic cell uptake experiment was carried out in vitro and showed that *Vps34*-deficient CD8α$^+$ DCs were less efficient than control DCs in phagocytosing apoptotic cells (Fig. 6 *C* and *D*). Thus, we concluded that *Vps34*-deficient CD8α$^+$ DCs are selectively defective in efferocytosis.

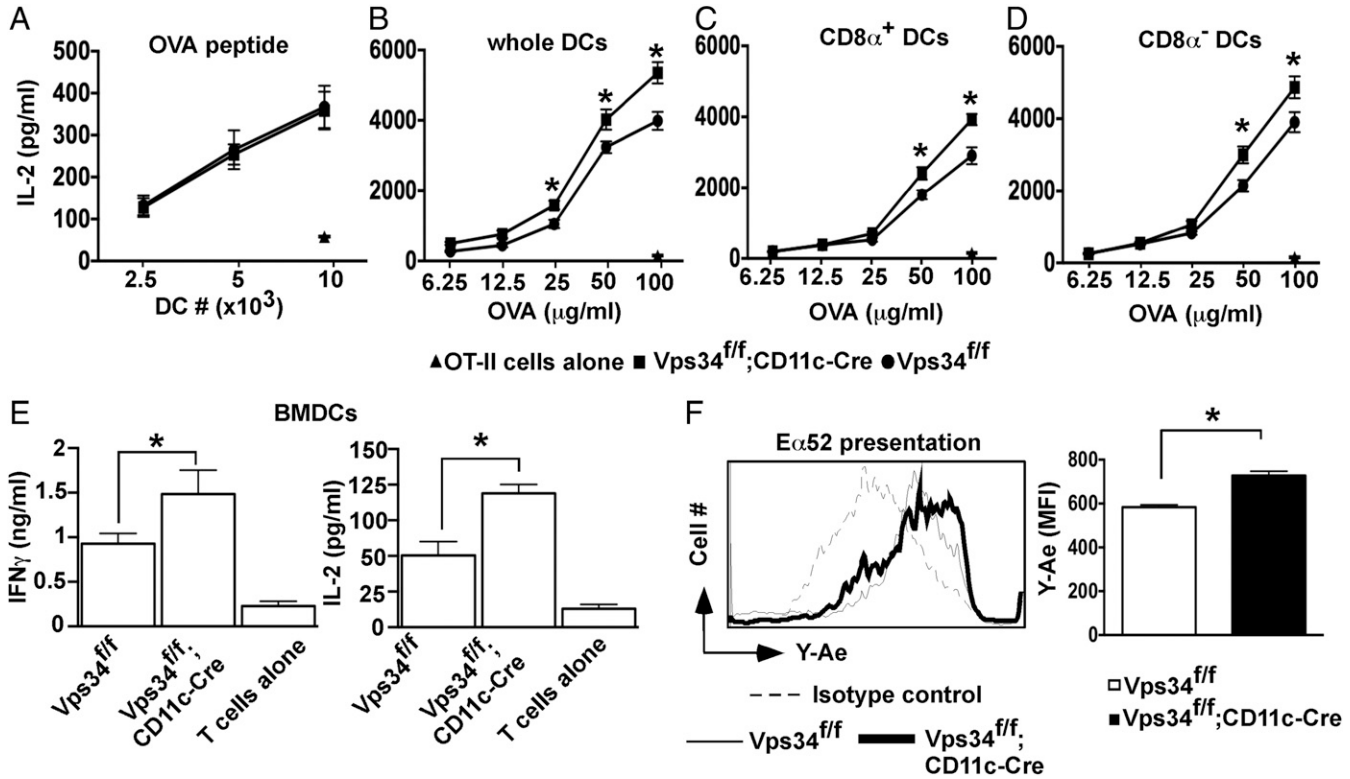

Fig. 4. Effects of *Vps34* deficiency on the MHC class II antigen-presentation pathway in DCs. (*A*) Sorted splenic DCs were pulsed with MHC class II-restricted OVA peptide for 1 h in complete medium and were washed. OT-II T cells were added, and culture supernatants were collected after 24 h to measure IL-2 by CBA. Representative plots from two experiments with four mice per group are shown. (*B*) Total splenic DCs (2×10^4) were cultured with OVA and 10^5 OT-II T cells, and culture supernatants were collected at 24 h for measurement of IL-2. Representative plots from two experiments with five mice per group are shown. Error bars indicate the means ± SD of triplicate wells. *$P < 0.05$. (*C* and *D*) Splenic CD8α$^+$ (*C*) and CD8α$^-$ (*D*) DCs were cultured with varying amounts of soluble OVA and OT-II T cells for 24 h, and IL-2 in the culture supernatant was measured. Representative graphs from three experiments with five mice per group are shown. Error bars indicate the means ± SD of triplicate wells. *$P < 0.05$. (*E*) BMDCs (10^4) were cultured with OVA (100 μg/mL) in the presence of OT-II cells (10^5). Culture supernatants were collected at 24 h, and IL-2 and IFNγ were measured by ELISA. Representative plots from two experiments with five mice per group are shown. Error bars indicate the means ± SD of triplicate wells. *$P < 0.05$. (*F*) BMDCs (2×10^5) were incubated with 50 μg/mL of GFP-Eα chimeric protein for 3 h, and cells were stained with YAe antibodies specific for Eα-derived $E\alpha_{52-68}$ peptide bound with I-A^b molecules. Representative plots from two experiments with four mice per group are shown. *$P < 0.05$.

DCs recognize "eat-me" signals on apoptotic cells via a variety of phagocytic receptors (21). Thus, we investigated mRNA expression of several of these receptors and found profoundly reduced expression of the T-cell Ig mucin (TIM)-4 receptor, but not of any other receptors investigated, on *Vps34*-deficient DCs (Fig. 6*E*). TIM-4, a receptor for phosphatidylserine, plays a critical role in the cross-presentation of apoptotic cells by phagocytes (22). We next tested surface expression of TIM-4 and found that CD8α$^+$ DCs expressed higher levels of TIM-4 receptor on the cell surface than did CD8α$^-$ DCs from either group of mice. Interestingly, TIM-4 expression was consistently reduced on *Vps34*-mutant CD8α$^+$ DCs compared with control DCs (Fig. 6 *F* and *G*). To rule out potential artifacts mediated by Cre expression, we analyzed *Vps34*$^{+/+}$;*CD11c-Cre* mice, which had a phenotype similar to the wild-type and *Vps34*$^{f/f}$ control animals used throughout these studies (Fig. S6), indicating that the observed defects were mediated by *Vps34* ablation.

We next performed experiments to determine whether reduced TIM-4 expression on DCs from *Vps34*$^{f/f}$;*CD11c-Cre* mice might be caused by the cytokines that are constitutively produced by these cells. For this purpose, we generated mixed bone marrow chimeras using *Vps34*$^{f/f}$;*CD11c-Cre*– and *Vps34*$^{f/f}$-derived donor cells and lethally irradiated wild-type recipient animals. The results showed that *Vps34*-deficient CD8α$^+$ DCs were reduced in prevalence compared with wild-type CD8α$^+$ DCs (Fig. 1*I*). Further, *Vps34*-deficient CD8α$^+$ DCs exhibited reduced TIM-4 expression and a reduced capacity to take up dead cells compared with wild-type CD8α$^+$ DCs (Fig. S7), indicating that the cytokines produced constitutively by *Vps34*-deficient CD8α$^+$ DCs fail to impair TIM-4 expression or the uptake of apoptotic cells by wild-type CD8α$^+$ DCs in vivo. This conclusion was supported by cocultures of DCs derived from *Vps34*$^{f/f}$;*CD11c-Cre* and *Vps34*$^{f/f}$ mice (1:1 ratio) for 24 h, which did not affect TIM-4 expression on either mutant or wild-type DCs (Fig. S8*A*). In a similar experiment, coculture of DCs from *Vps34*$^{f/f}$;*CD11c-Cre* mice and whole splenocytes derived from *Vps34*$^{f/f}$ mice failed to influence TIM-4 expression on *Vps34* mutant DCs (Fig. S8 *B* and *C*). We also considered that IL-10, one of the immunosuppressive cytokines spontaneously produced by *Vps34*-deficient DCs (Fig. 2), may potentially impact TIM-4 expression, but we found that IL-10 treatment had no effect on TIM-4 expression by wild-type DCs (Fig. S8*D*).

In an attempt to provide direct evidence for reduced TIM-4 expression as a cause of defective efferocytosis by *Vps34*-deficient DCs, we transfected these cells with a TIM-4–containing expression vector, but, as was consistent with similar attempts to transfect primary DCs by other investigators (23), we were unsuccessful. As an alternative approach, we used the DC2.4 cell line (24) and primary BMDCs, which lack TIM-4 expression (Fig. 6 *H* and *I*). Transfection with the TIM-4 expression vector resulted in efficient TIM-4 surface expression, which in turn enhanced the uptake of apoptotic cells (Fig. 6 *H* and *I*), demonstrating that TIM-4 can function as a phagocytic receptor for apoptotic cells on DCs. Although these findings point to blunted TIM-4 expression as a likely defect in *Vps34*-deficient DCs evoking defective efferocytosis, they do not exclude the possibility that other phagocytic receptors are involved.

DC Defects Are Independent of Light Chain 3-Associated Phagocytosis. The Beclin1–Vps34 complex is used by the canonical autophagy process as well as by light chain 3 (LC3)-associated phagocytosis (LAP) (25). The protein Rubicon is critically required for LAP but not for canonical autophagy (26). Therefore, we analyzed DCs from *Rubicon*-deficient mice, which exhibited normal prevalence of the CD8α$^+$ subset (Fig. 7 *A* and *B*), lack of constitutive cytokine production (Fig. 7*C*), normal TIM-4 surface expression (Fig. 7*D*), and a normal capacity to take up dead cells (Fig. 7*E*). These results indicate that the alterations in CD8α$^+$ DCs observed in *Vps34*-mutant mice are most likely not caused by defective noncanonical autophagy. Instead, electron microscopy studies revealed autophagosomal double-membrane structures, indicating defective canonical autophagy, in wild-type but not *Vps34*-deficient DCs (Fig. S9*A*). To provide further support for defects in canonical autophagy in *Vps34*-deficient DCs, we measured mitochondrial and endoplasmic reticulum (ER) mass, which was enhanced in *Vps34*-deficient compared with wild-type DCs (Fig. S9*B*). Although these findings are consistent with the premise that the observed phenotypes in *Vps34*-deficient DCs are mediated by defects in canonical autophagy, we cannot exclude a role for other cellular processes in which Vps34 is involved.

Defective Induction of Responses to Apoptotic Cell-Associated Antigens. To investigate the functional consequences of *Vps34* ablation in DCs on the induction of an immune response, we

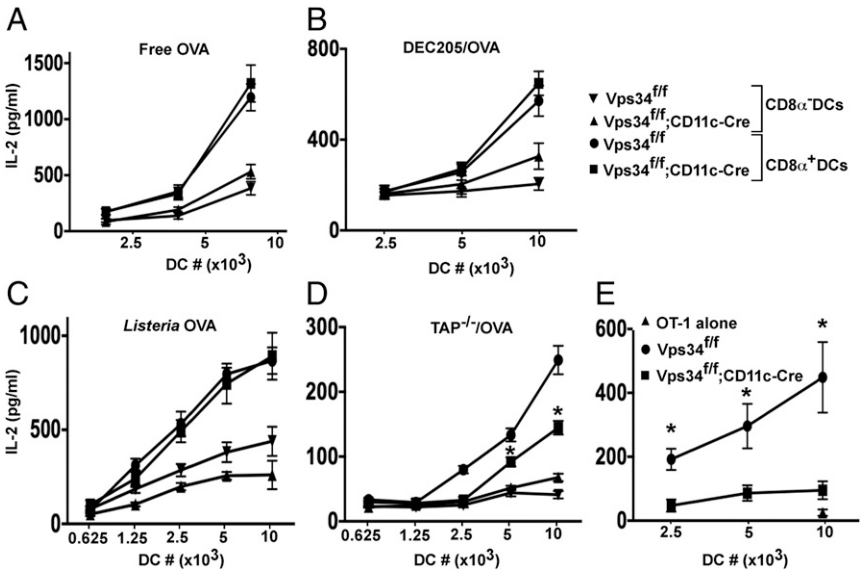

Fig. 5. Cross-presentation of MHC class I antigens by *Vps34*-deficient DCs. (*A*) Splenic CD8α$^+$ and CD8α$^-$ DCs (10^4 cells) were cultured with varying amounts (62.5–250 μg/mL) of free OVA and 2×10^5 OT-I T cells for 24 h. Supernatants were collected, and IL-2 was measured by CBA. (*B*) Splenic CD8α$^+$ and CD8α$^-$ DCs (10^6 cells) were incubated with biotin-labeled anti-DEC205 antibodies followed by streptavidin-OVA delivery reagent and were cultured in the presence of 2×10^5 OT-I T cells for 24 h. Supernatants were collected for measurement of IL-2 by CBA. (*C*) Splenic CD8α$^+$ and CD8α$^-$ DCs were cultured with OVA-expressing *L. monocytogenes* and 2×10^5 OT-I T cells for 24 h. Supernatants were used to measure IL-2 by CBA. (*D*) *TAP*$^{-/-}$ splenocytes were intracellularly loaded with OVA, sublethally irradiated, and cultured with splenic CD8α$^+$ or CD8α$^-$ DCs. OT-I T cells (2×10^5) were added and were cultured for 24 h. Supernatants were collected to measure IL-2 by CBA. In *A*–*D*, graphs are representative of three individual experiments with five mice per group. Error bars indicate the means ± SD of triplicate wells. *$P <$ 0.05. (*E*) Mice were injected with 20×10^6 apoptotic *TAP*$^{-/-}$ splenocytes loaded intracellularly with OVA by osmotic shock. After 2 h, splenocytes were prepared, and DCs were purified and cultured in the presence of OT-I T cells for 24 h. The culture supernatants were collected to measure IL-2 by CBA. Error bars indicate the mean ± SEM for five mice. *$P < 0.05$.

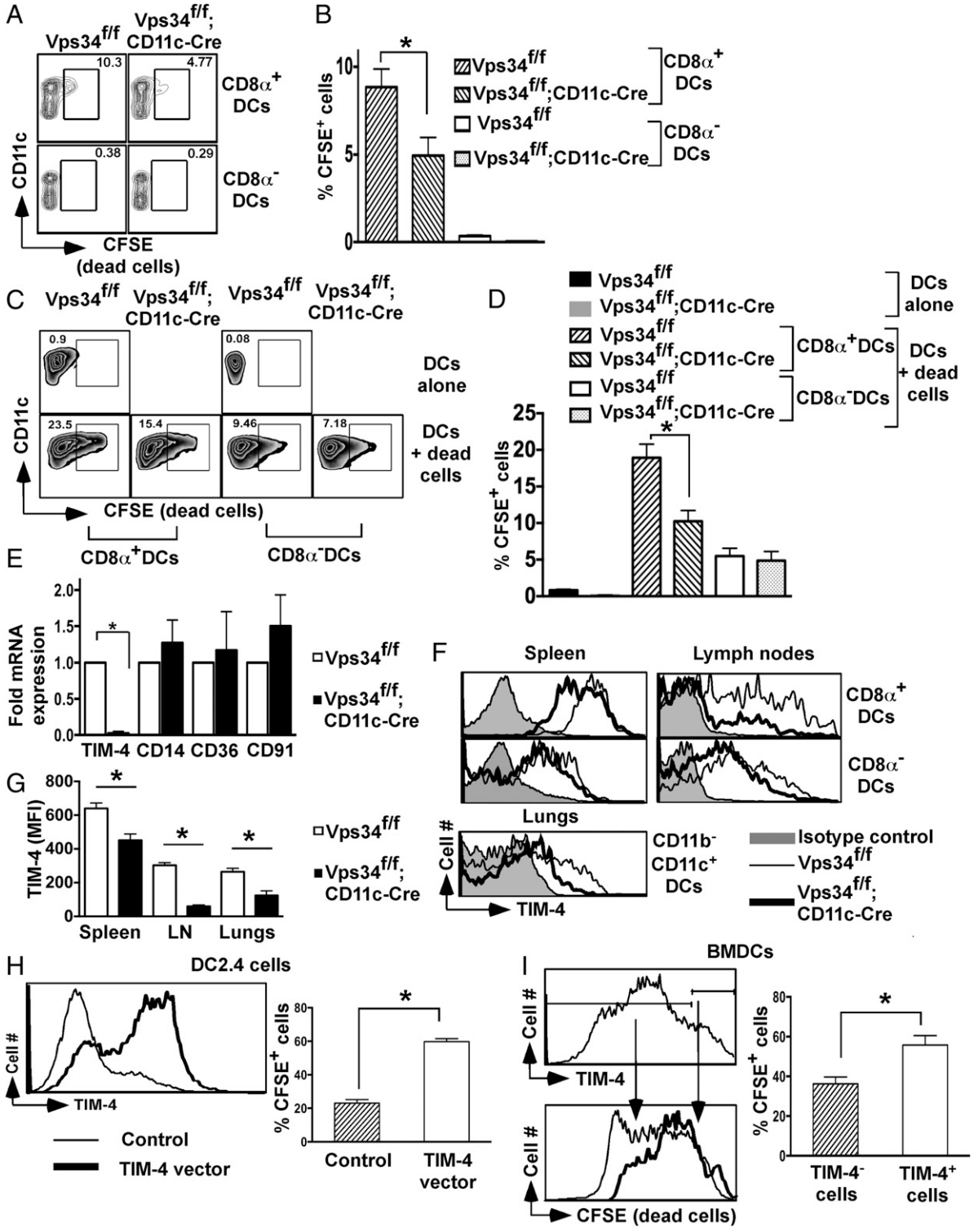

Fig. 6. *Vps34*-deficient DCs have defects in the uptake of cell corpses and TIM-4 expression. (*A*) For in vivo uptake of apoptotic cells by DCs, 3×10^7 CFSE-labeled apoptotic B6.SJL ($CD45.1^+$) splenocytes were injected into groups of mice. After 4 h spleen cells were prepared, and $CFSE^+CD45.1^-CD45.2^+$ DCs subsets were determined. A representative plot is shown. (*B*) A summary of the experiment in *A* is shown. Data are pooled from two individual experiments (five mice in each group). $^*P < 0.05$. (*C*) CFSE-labeled apoptotic cells ($CD45.1^+$) were incubated with total DCs ($CD45.2^+$) derived from the indicated mice for 3 h (1:10 ratio). At the end of the culture, $CFSE^+CD45.1^-CD45.2^+$ DC subsets were determined as shown. (*D*) A summary of the experiment in *C* is shown. Data are pooled from two individual experiments (five mice in each group). $^*P < 0.01$. (*E*) mRNA expression of the indicated phagocytic receptors in splenic DCs. Data shown are representative of three independent experiments. $^*P < 0.01$. (*F*) Expression of TIM-4 on DC subsets. (*G*) The mean fluorescence intensity (MFI) of TIM-4 expression shown in *F* is summarized. Data are pooled for six mice from two individual experiments. $^*P < 0.01$. (*H* and *I*) DC2.4 cells (*H*) or BMDCs (*I*) were transfected with a TIM-4-containing vector, $CFSE^+$ apoptotic cells were added 24 h later, and 3 h later cells were stained with an anti–TIM-4 antibody and were analyzed by flow cytometry. $^*P < 0.05$. (*I*) A summary of the experiment in *H*. Four independent transfection experiments were performed.

measured CTL responses to cell corpse-associated antigens in vivo. Sublethally irradiated, OVA-loaded *TAP*$^{-/-}$ splenocytes were injected into mice, and 7 d later we measured $OVA_{257–264}$-specific CTL responses. Consistent with the relative reduction of CD8α$^+$ DCs in spleens of *Vps34*$^{f/f}$;*CD11c-Cre* mice and defects in the cross-presentation of apoptotic cells (Fig. 5*E*), the results showed efficient induction of OVA-specific CTLs in *Vps34*$^{f/f}$ mice but a blunted response in *Vps34*$^{f/f}$;*CD11c-Cre* mice (Fig. 8).

Enhanced B16 Lung Melanoma Metastases. Recent studies on CD8α$^+$ DCs have shown that these DCs have a critical role in cross-presenting tumor-associated antigens and in inducing tumor-specific CTLs (27). We therefore challenged *Vps34*$^{f/f}$;*CD11c-Cre* and *Vps34*$^{f/f}$ mice with B16 melanoma cells and scored the animals 15–17 d later for lung tumor metastases. *Vps34*$^{f/f}$;*CD11c-Cre* mice possessed significantly higher tumor burdens than *Vps34*$^{f/f}$ control mice (Fig. 9).

CD11b$^-$CD11c^{hi} DCs in the lungs are developmentally related to splenic CD11c$^+$CD8α$^+$CD103$^+$ DCs (16). This population of DCs in the lungs was recently shown to be critically required for preventing B16 lung metastases (28). We therefore analyzed distinct lung myeloid cell populations and found high TIM-4 expression on CD11b$^-$CD11c^{hi} DCs from wild-type mice but not on those from *Vps34*$^{f/f}$;*CD11c-Cre* mice (Fig. S10*A*). These results suggest that the TIM-4–expressing CD11b$^-$CD11c^{hi} population of DCs in the lungs plays a role in controlling tumor metastasis.

We considered the possibility that the increased tumor burden in *Vps34*$^{f/f}$;*CD11c-Cre* mice may be related to spontaneous cytokine production by DCs in these animals. We therefore evaluated CD11b$^+$Gr1$^+$ myeloid-derived suppressor cells, which promote tumor growth and are induced in response to inflammatory stimuli (29), but found no difference in the frequency of these cells in mutant and wild-type animals (Fig. S10*B*).

Discussion

The class III PI3K Vps34 plays a role in endocytosis, intracellular vesicular trafficking, and autophagy, key processes that control the presentation of self and foreign antigens by DCs to naive T lymphocytes. Here we analyzed DC functions in mice with a DC-specific *Vps34* gene ablation. DCs from these animals exhibited a decrease in the ratio of CD8α$^+$ to CD8α$^-$ subsets that was cell intrinsic and mediated by impaired DC homeostasis. Although the frequency of CD8α$^+$ DCs was reduced in *Vps34*$^{f/f}$;*CD11c-Cre* mice, these cells retained their capacity to cross-present the model antigen OVA to MHC class I-restricted T cells when delivered in a soluble form through the DEC205 receptor and via expression in bacteria but were profoundly impaired in their capacity to cross-present OVA antigens associated with dying cells. This impaired capacity was associated with reduced expression of TIM-4, a receptor predominantly expressed by CD8α$^+$ DCs that binds with phosphatidylserine to engulf apoptotic cells (22, 27). Therefore, the combined defect in the homeostatic maintenance of CD8α$^+$ DCs and blunted efferocytosis in *Vps34*$^{f/f}$;*CD11c-Cre* mice resulted in impaired induction of CTL responses to antigens associated with dying cells and defective antimetastatic immunity. Although our findings suggest defective TIM-4 expression as a likely cause for the impaired efferocytosis by *Vps34*-deficient DCs, additional phagocytic receptors for apoptotic cells may be involved.

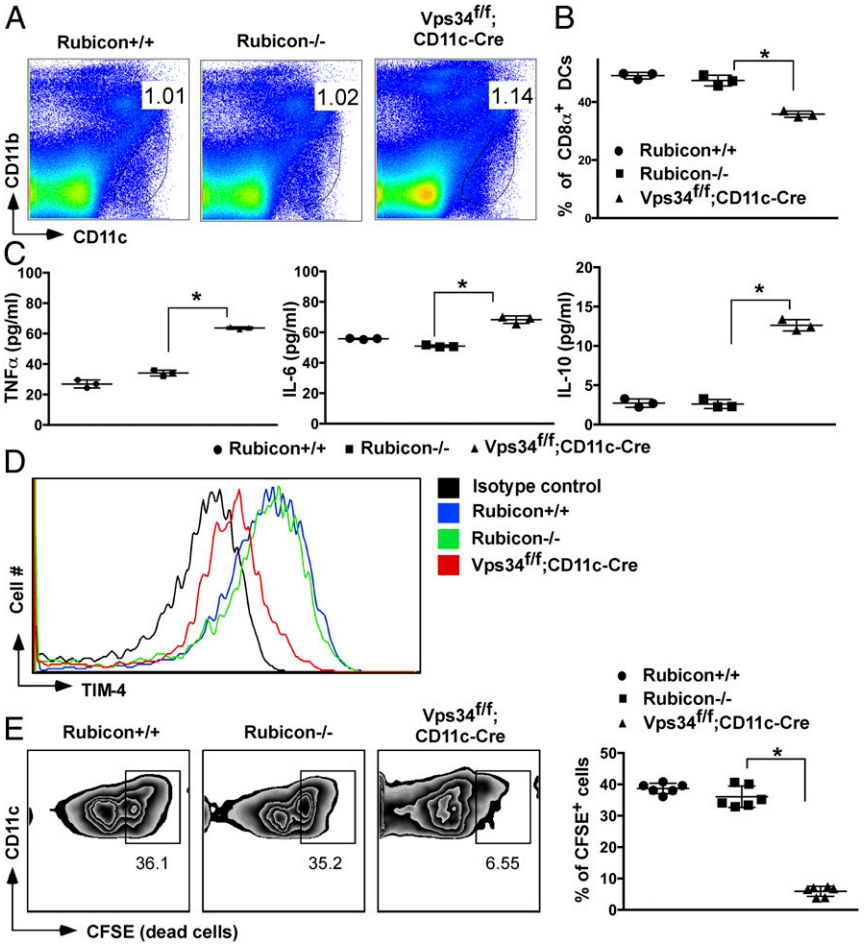

Fig. 7. DCs in *Rubicon*-deficient mice. (*A*) Frequency of total splenic DCs. (*B*) Percentage of splenic CD8α$^+$ DCs. The data are representative of 10 mice in each experimental group. (*C*) Splenic DCs from the indicated groups of mice were purified by FACS and cultured for 24 h. Culture supernatants were collected to measure TNFα, IL-6, and IL-10 by CBA. An experiment representative of three individual experiments is shown. The error bars indicate the means ± SD of triplicate wells. (*D*) Expression of TIM-4 on splenic CD8α$^+$ DCs. An experiment representative of three individual experiments is shown. (*E*) Dead cell uptake of CD8α$^+$ or CD8α$^-$ DCs derived from the indicated mice as described in the legend of Fig. 6*C* is shown (*Left*) with a summary of six mice from each experimental group (*Right*). *$P < 0.05$.

In addition to autophagy, Vps34 plays a role in endocytosis (9, 30). Our findings showed that DCs from *Vps34*$^{f/f}$;*CD11c-Cre* mice lack significant defects in endocytosis or phagocytosis but exhibit abnormalities in autophagosomal double-membrane structures and mitochondrial ER mass, suggesting defective autophagy as the main process responsible for the observed alterations in DC functions.

Vps34 has been implicated in both canonical and noncanonical autophagy (31). During the induction of canonical autophagy the preinitiation complex triggers recruitment of the Beclin1–Vps34 complex, followed by induction of Vps34 kinase activity, recruitment of multiple Atg proteins, and lipidation of LC3. This process allows the formation of double-membrane autophagosomal structures, which ultimately fuse with lysosomes to degrade the contents of the autophagosomes (9). In our previous studies we demonstrated that deletion of *Vps34* in T cells, heart, or liver results in profound defects in canonical autophagy and in the loss of normal cellular function in vivo (11, 13). *Vps34* deficiency in DCs similarly caused defects in canonical autophagy, resulting in the complete loss of visible double-membrane autophagosomal structures, the accumulation of cellular organelles, and increases in ER and mitochondrial mass. In the noncanonical autophagy pathway, TLR activation induces the recruitment of several Atg proteins such as LC3 to a single-membrane phagosome. Such LC3-enriched phagosomes degrade their contents more efficiently and thus modulate immune responses triggered by the engulfed cargo (32). This process of noncanonical autophagy, also known as "LAP," requires the activity of the Beclin1–Vps34 complex before recruitment of LC3 to phagosomes (33, 34). A recent study has demonstrated that the Vps34 complex is critically required for the induction of LAP and for canonical autophagy in macrophages (26). Therefore the spontaneous activation and cytokine secretion by *Vps34*-deficient DCs may be potentially attributed to deficiencies in the anti-inflammatory activity of canonical autophagy, to LAP, or to both. Our results with mice deficient in Rubicon, which binds Vps34 and is required for LAP but not for canonical autophagy (26), suggest that defects in *Vps34*-deficient DCs are not caused by defective LAP. Although these findings are consistent with defective canonical autophagy being the cause of the observed phenotype of *Vps34*-deficient DCs, defects in additional cellular processes that involve Vps34 may contribute as well.

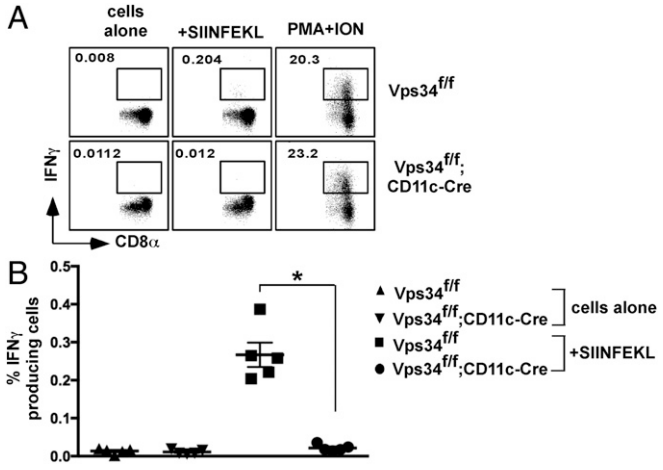

Fig. 8. Defective CTL responses to dead cell-associated antigens in *Vps34*$^{f/f}$;*CD11c-Cre* mice. The indicated mice were immunized with apoptotic, OVA-loaded *TAP*$^{-/-}$ splenocytes. Seven days later, spleen cells were stimulated with or without $OVA_{257–264}$ peptide for 6 h, and IFN-γ–producing $CD8^+$ T cells were detected by flow cytometry. As a control, cells were stimulated with phorbol myristate acetate plus ionomycin (PMA +ON). Representative flow cytometry plots from two individual experiments (*A*) and a summary of the percentage of IFN-γ^+CD8^+ cells (*B*) are shown; $n = 5$ per group. $^*P < 0.01$.

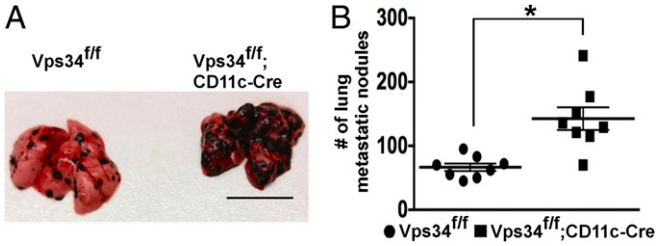

Fig. 9. Enhanced B16 melanoma metastases in mice with a DC-specific *Vps34* ablation. Mice were challenged i.v. with 3×10^5 B16 melanoma cells, and 15–17 d later the numbers of metastatic nodules in the lungs were counted. (*A*) Representative images. (Scale bar, 1 cm.) (*B*) Results from two independent experiments were pooled and plotted as the mean ± SEM of seven mice per group. $^*P < 0.05$.

Autophagy has been shown to play a role in processing antigens for presentation to MHC class I- and class II-restricted T cells (4). Surprisingly, we found enhanced antigen presentation via the conventional MHC class I and class II pathways by *Vps34*-deficient DCs. Our electron microscopic analyses of *Vps34*-deficient DCs revealed increased accumulation of ER membranes. Such an expanded ER compartment, rich in the components of the MHC class I processing machinery, may allow efficient processing of cytosolic proteins for presentation onto MHC class I-restricted T cells. Thus, a combination of factors, including increased sensitivity of partially activated *Vps34*-deficient DCs to IFN-γ stimulation, together with defects in autophagy resulting in an expansion of the MHC class I peptide-loading compartment, may contribute to the observed enhancement in MHC class I-restricted antigen presentation. In professional APCs such as DCs, MHC class II-presented antigens reach phagosomes via endocytosis or pinocytosis. These phagosomes then fuse with MHC class II-containing endosomal compartments in which the antigens are degraded and peptides are loaded onto MHC class II-restricted T cells (35). Although our results showed enhanced MHC class II-restricted antigen presentation by *Vps34*-deficient DCs, we found a modest defect rather than enhancement in the uptake of antigens by *Vps34*-deficient DCs. A recent study provided evidence that autophagosomal vesicles constantly fuse with the MHC class II peptide-loading compartment and facilitate antigen presentation (36). The increased accumulation of electron-dense lysosomal structures observed in *Vps34*-deficient DCs might explain the enhanced MHC class II-restricted antigen presentation.

Targeting Vps34 to inhibit autophagy has recently been considered as an anticancer therapy (37). Autophagy protects cancer cells against metabolic stress such as nutrient starvation and hypoxic conditions. Inhibiting autophagy in cancer cells therefore may reduce resistance to chemotherapy and radiation therapy. A selective Vps34 inhibitor, SAR405, in combination with the mammalian target of rapamycin (mTOR) inhibitor everolimus, was shown to inhibit the proliferation of renal tumor cell lines in vitro (38). Our results suggest that Vps34 inhibition may lead to impaired T-cell–mediated immunity in tumors that may limit the utility of SAR405 in cancer therapy.

Materials and Methods

Reagents, electron microscopy, analyses of mitochondrial and ER stress, Western blotting, lung cell preparation, DC activation experiments, antigen-presentation assays, endocytosis and phagocytosis assays, quantitative real-time PCR, TIM-4 overexpression, and induction of lung metastases are described in *SI Materials and Methods*.

Mice. *Vps34*$^{f/f}$ (11, 13), *Rubicon*$^{-/-}$ (26), and *TAP*$^{-/-}$ (39) mice have been described. *CD11c-Cre*, OT-I, and OT-II transgenic mice were obtained from The Jackson Laboratory. All mice were housed under specific pathogen-free conditions and in compliance with guidelines from the Institutional Animal Care and Use Committee at Vanderbilt University.

Isolation of Splenic DCs and Generation of BMDCs. Spleens were treated with 0.2 mg/mL of collagenase D and DNase I for 15–20 min in plain Roswell Park Memorial Institute (RPMI) medium at 37 °C. DCs were purified based on the expression of CD11c and MHC class II using FACS as described previously (40), at a final purity greater than 75%. CD8α microbeads (Miltenyi Biotec) were used to sort $CD8\alpha^+$ DCs, and the remaining cells were used as $CD8\alpha^-$ DCs. BMDCs were generated using recombinant GM-CSF as described (41, 42). For Flt3L-driven BMDCs, 1.5×10^6 bone marrow cells/mL were cultured in 4 mL of complete medium for 9 d in the presence of 150 ng/mL of recombinant FMS-like tyrosine kinase-3 ligand (rFlt3L) as described (43).

In Vitro and in Vivo Phagocytosis of Cell Corpses. In vitro and in vivo dead cell uptake assays were performed as described (44), with sublethally irradiated, carboxyfluorescein succinimidyl ester (CFSE)-labeled B6.SJL (CD45.1) splenocytes. For in vitro assays apoptotic cells were incubated with DCs (CD45.2) for 3 h at a 1:10 ratio in U-bottomed plates. The cells were washed, and $CFSE^+$ cells among $CD45.2^+CD45.1^-$ cells were examined by flow cytometry. For in vivo assays, CFSE-labeled apoptotic cells were injected into mice (3×10^7 cells per mouse), and after 4 h spleen cells were prepared and $CFSE^+$ DCs among $CD45.2^+CD45.1^-$ cells were examined.

In Vivo $CD8^+$ T-Cell Responses. Splenocytes from $TAP^{-/-}$ mice were loaded with 10 mg/mL OVA by osmotic shock, irradiated sublethally, and washed, and mice were injected with 2×10^7 cells per mouse. Seven days later, mice were killed, splenocytes were cultured with 1 μM $OVA_{257–264}$ peptide for 6 h in the presence of Brefeldin A, and intracellular IFN-γ levels in $CD8^+$ T cells were detected by flow cytometry.

Generation of Bone Marrow Chimeras. B6 (CD45.2) mice were lethally irradiated (1,000 cGy) and 6 h later were injected with 10^7 bone marrow cells derived from wild-type B6.SJL (CD45.1) and $Vps34^{f/f}$;*CD11c-Cre* or $Vps34^{f/f}$ (CD45.2) mice mixed at a 1:1 ratio. Mice were used for experiments at 12 wk after injection of bone marrow cells.

Statistical Analyses. Statistical significance was determined by an unpaired two-tailed Student *t* test or one-way ANOVA using GraphPad Prism software; $P < 0.05$ was considered significant.

ACKNOWLEDGMENTS. We thank Drs. Randy Brutkiewicz, Marc Jenkins, Danyvid Olivares-Villagómez, Kenneth Rock, Nilabh Shastri, Chyung-Ru Wang, John Wilson, and Keith Wilson for providing reagents. FACS sorting was performed in the Flow Cytometry Shared Resource at Vanderbilt University Medical Center, supported by the Vanderbilt Ingram Cancer Center Support Grant P30 CA68485 and Vanderbilt Digestive Disease Research Center Grant DK058404. This work was supported by NIH Grants DK104817 (to L.V.K.), DK081536 (to L.W. and L.V.K.), and NS064090 (to J.Z.), a Veterans Administration Merit Award (to J.Z.), the National Multiple Sclerosis Society (L.V.K.), and the Crohn's and Colitis Foundation of America (L.V.K.).

1. Vyas JM, Van der Veen AG, Ploegh HL (2008) The known unknowns of antigen processing and presentation. *Nat Rev Immunol* 8:607–618.
2. Cresswell P, Ackerman AL, Giodini A, Peaper DR, Wearsch PA (2005) Mechanisms of MHC class I-restricted antigen processing and cross-presentation. *Immunol Rev* 207: 145–157.
3. Bevan MJ (2006) Cross-priming. *Nat Immunol* 7:363–365.
4. Romao S, Gannage M, Münz C (2013) Checking the garbage bin for problems in the house, or how autophagy assists in antigen presentation to the immune system. *Semin Cancer Biol* 23:391–396.
5. Yang Z, Klionsky DJ (2010) Mammalian autophagy: Core molecular machinery and signaling regulation. *Curr Opin Cell Biol* 22:124–131.
6. Mizushima N (2007) Autophagy: Process and function. *Genes Dev* 21:2861–2873.
7. Yorimitsu T, Klionsky DJ (2005) Autophagy: Molecular machinery for self-eating. *Cell Death Differ* 12:1542–1552.
8. Nikoletopoulou V, Papandreou ME, Tavernarakis N (2015) Autophagy in the physiology and pathology of the central nervous system. *Cell Death Differ* 22:398–407.
9. Funderburk SF, Wang QJ, Yue Z (2010) The Beclin 1-VPS34 complex–At the crossroads of autophagy and beyond. *Trends Cell Biol* 20:355–362.
10. Backer JM (2008) The regulation and function of class III PI3Ks: Novel roles for Vps34. *Biochem J* 410:1–17.
11. Parekh VV, et al. (2013) Impaired autophagy, defective T cell homeostasis, and a wasting syndrome in mice with a T cell-specific deletion of Vps34. *J Immunol* 190: 5086–5101.
12. Willinger T, Flavell RA (2012) Canonical autophagy dependent on the class III phosphoinositide-3 kinase Vps34 is required for naive T-cell homeostasis. *Proc Natl Acad Sci USA* 109:8670–8675.
13. Jaber N, et al. (2012) Class III PI3K Vps34 plays an essential role in autophagy and in heart and liver function. *Proc Natl Acad Sci USA* 109:2003–2008.
14. Zhou X, et al. (2010) Deletion of PIK3C3/Vps34 in sensory neurons causes rapid neurodegeneration by disrupting the endosomal but not the autophagic pathway. *Proc Natl Acad Sci USA* 107:9424–9429.
15. Kihara A, Noda T, Ishihara N, Ohsumi Y (2001) Two distinct Vps34 phosphatidylinositol 3-kinase complexes function in autophagy and carboxypeptidase Y sorting in *Saccharomyces cerevisiae*. *J Cell Biol* 152:519–530.
16. Edelson BT, et al. (2010) Peripheral CD103+ dendritic cells form a unified subset developmentally related to CD8alpha+ conventional dendritic cells. *J Exp Med* 207:823–836.
17. Sung SS, et al. (2006) A major lung CD103 (alphaE)-beta7 integrin-positive epithelial dendritic cell population expressing Langerin and tight junction proteins. *J Immunol* 176:2161–2172.
18. Naik SH, et al. (2005) Cutting edge: Generation of splenic CD8+ and CD8- dendritic cell equivalents in Fms-like tyrosine kinase 3 ligand bone marrow cultures. *J Immunol* 174:6592–6597.
19. Pittini Á, Casaravilla C, Allen JE, Díaz Á (2016) Pharmacological inhibition of PI3K class III enhances the production of pro- and anti-inflammatory cytokines in dendritic cells stimulated by TLR agonists. *Int Immunopharmacol* 36:213–217.
20. den Haan JM, Lehar SM, Bevan MJ (2000) CD8(+) but not CD8(-) dendritic cells cross-prime cytotoxic T cells in vivo. *J Exp Med* 192:1685–1696.
21. Ravichandran KS, Lorenz U (2007) Engulfment of apoptotic cells: Signals for a good meal. *Nat Rev Immunol* 7:964–974.
22. Miyanishi M, et al. (2007) Identification of Tim4 as a phosphatidylserine receptor. *Nature* 450:435–439.
23. Smyth Templeton NE (2015) *Gene Therapy and Cell Therapy* (CRC, Boca Raton, FL).
24. Shen Z, Reznikoff G, Dranoff G, Rock KL (1997) Cloned dendritic cells can present exogenous antigens on both MHC class I and class II molecules. *J Immunol* 158:2723–2730.
25. Boyle KB, Randow F (2015) Rubicon swaps autophagy for LAP. *Nat Cell Biol* 17: 843–845.
26. Martinez J, et al. (2015) Molecular characterization of LC3-associated phagocytosis reveals distinct roles for Rubicon, NOX2 and autophagy proteins. *Nat Cell Biol* 17:893–906.
27. Hildner K, et al. (2008) Batf3 deficiency reveals a critical role for CD8alpha+ dendritic cells in cytotoxic T cell immunity. *Science* 322:1097–1100.
28. Headley MB, et al. (2016) Visualization of immediate immune responses to pioneer metastatic cells in the lung. *Nature* 531:513–517.
29. Ostrand-Rosenberg S, Sinha P (2009) Myeloid-derived suppressor cells: Linking inflammation and cancer. *J Immunol* 182:4499–4506.
30. Backer JM (2016) The intricate regulation and complex functions of the class III phosphoinositide 3-kinase Vps34. *Biochem J* 473:2251–2271.
31. Mehta P, Henault J, Kolbeck R, Sanjuan MA (2014) Noncanonical autophagy: One small step for LC3, one giant leap for immunity. *Curr Opin Immunol* 26:69–75.
32. Münz C (2015) Of LAP, CUPS, and DRibbles - unconventional use of autophagy proteins for MHC restricted antigen presentation. *Front Immunol* 6:200.
33. Sanjuan MA, et al. (2007) Toll-like receptor signalling in macrophages links the autophagy pathway to phagocytosis. *Nature* 450:1253–1257.
34. Martinez J, et al. (2011) Microtubule-associated protein 1 light chain 3 alpha (LC3)-associated phagocytosis is required for the efficient clearance of dead cells. *Proc Natl Acad Sci USA* 108:17396–17401.
35. Roche PA, Furuta K (2015) The ins and outs of MHC class II-mediated antigen processing and presentation. *Nat Rev Immunol* 15:203–216.
36. Schmid D, Pypaert M, Münz C (2007) Antigen-loading compartments for major histocompatibility complex class II molecules continuously receive input from autophagosomes. *Immunity* 26:79–92.
37. Choi AM, Ryter SW, Levine B (2013) Autophagy in human health and disease. *N Engl J Med* 368:1845–1846.
38. Ronan B, et al. (2014) A highly potent and selective Vps34 inhibitor alters vesicle trafficking and autophagy. *Nat Chem Biol* 10:1013–1019.
39. Van Kaer L, Ashton-Rickardt PG, Ploegh HL, Tonegawa S (1992) TAP1 mutant mice are deficient in antigen presentation, surface class I molecules, and CD4-8+ T cells. *Cell* 71:1205–1214.
40. Lee HK, et al. (2010) In vivo requirement for Atg5 in antigen presentation by dendritic cells. *Immunity* 32:227–239.
41. Lutz MB, et al. (1999) An advanced culture method for generating large quantities of highly pure dendritic cells from mouse bone marrow. *J Immunol Methods* 223:77–92.
42. Yan J, et al. (2006) In vivo role of ER-associated peptidase activity in tailoring peptides for presentation by MHC class Ia and class Ib molecules. *J Exp Med* 203:647–659.
43. Brasel K, De Smedt T, Smith JL, Maliszewski CR (2000) Generation of murine dendritic cells from flt3-ligand-supplemented bone marrow cultures. *Blood* 96:3029–3039.
44. Lorenzi S, et al. (2011) Type I IFNs control antigen retention and survival of CD8α(+) dendritic cells after uptake of tumor apoptotic cells leading to cross-priming. *J Immunol* 186:5142–5150.
45. Moore MW, Carbone FR, Bevan MJ (1988) Introduction of soluble protein into the class I pathway of antigen processing and presentation. *Cell* 54:777–785.
46. Lewis MD, et al. (2015) A reproducible method for the expansion of mouse CD8+ T lymphocytes. *J Immunol Methods* 417:134–138.
47. Van Kaer L, et al. (2014) $CD8\alpha\alpha^+$ innate-type lymphocytes in the intestinal epithelium mediate mucosal immunity. *Immunity* 41:451–464.
48. Parekh VV, et al. (2005) Glycolipid antigen induces long-term natural killer T cell anergy in mice. *J Clin Invest* 115:2572–2583.